

## A Model of Low-Mass Neutron Stars with a Quark Core

G. B. Alaverdyan, A. R. Arutyunyan\*, and Yu. L. Vartanyan

*Yerevan State University, Alex Manoogian ul. 1, Yerevan, 375049 Armenia*

Received May 18, 2001; in final form, August 27, 2001

**Abstract**—We consider an equation of state that leads to a first-order phase transition from the nucleon state to the quark state with a transition parameter  $\lambda > 3/2$  ( $\lambda = \rho_Q/(\rho_N + P_0/c^2)$ ) in superdense nuclear matter. Our calculations of integrated parameters for superdense stars using this equation of state show that on the stable branch of the dependence of stellar mass on central pressure ( $dM/dP_c > 0$ ) in the range of low masses, a new local maximum with  $M_{\max} = 0.082M_\odot$  and  $R = 1251$  km appears after the formation of a toothlike kink ( $M = 0.08M_\odot$ ,  $R = 205$  km) attributable to quark production. For such a star, the mass and radius of the quark core are  $M_{\text{core}} = 0.005M_\odot$  and  $R_{\text{core}} = 1.73$  km, respectively. In the model under consideration, mass accretion can result in two successive transitions to a quark-core neutron star with energy release similar to a supernova explosion: initially, a low-mass star with a quark core is formed; the subsequent accretion leads to configurations with a radius of  $\sim 1000$  km; and, finally, the second catastrophic restructuring gives rise to a star with a radius of  $\sim 100$  km.

© 2002 MAIK “Nauka/Interperiodica”.

Key words: *low-mass neutron stars, equations of state for superdense matter*

### INTRODUCTION

Given the possible formation of strange quark matter in superdense nuclear plasma (Witten 1984; Farhi and Jaffe 1984), the equation of state for superdense matter assumes the Van der Waals form. In this case, it turns out that, depending on the insufficiently accurate parameters in the strong interaction theory, the energy per baryon  $\varepsilon$  as a function of the baryon density  $n$  can have a negative and positive minimum,  $\varepsilon_{\min}$ . In turn, this circumstance leads to two alternatives.

For  $\varepsilon_{\min} < 0$ , a self-bound state of strange quark matter and, as a result, self-confined configurations that are entirely composed of such matter, the so-called “strange stars” studied by Alcock *et al.* (1986), Haensel *et al.* (1986), Kondratyuk *et al.* (1990), Weber and Glendenning (1992), and Vartanyan *et al.* (1995), are possible. For an equation of state with  $\varepsilon_{\min} > 0$  and at densities above the threshold for the production of strange quark matter, a first-order phase transition with a density discontinuity takes place. In this case, according to the Gibbs condition (or the Maxwell construction), a thermodynamic equilibrium between the quark matter and the nucleon component is possible; i.e., the two phases coexist. The models with this equation of state have a core composed of strange quark matter and an envelope with the composition of matter of

ordinary neutron stars; there is a density discontinuity at the interface.

In many studies, apart from those mentioned above, models of strange stars were computed and comprehensively analyzed (Martem'yanov 1994; Khadkikar *et al.* 1995; Heiselberg and Hjorth-Jensen 1999; and references therein). However, much fewer studies are devoted to configurations with a density discontinuity (Haensel 1986; Carinhas 1993; Alaverdyan *et al.* 1995). Noteworthy are the most complete calculations (Heiselberg *et al.* 1993; Lorenz *et al.* 1993; Glendenning 1997) of models with a mixed phase, which contain various quark configurations in the form of droplet, rodlike, and platelike structures; these models assume continuous pressure and density variations in the quark-phase formation region (Glendenning *et al.* 1992). The results of these authors show that the formation of the mixed phase of quark and nuclear matter may be energetically more or less favorable than an ordinary first-order nucleon-to-quark phase transition, depending on the local surface and Coulomb energies associated with the formation of mixed-phase quark and nuclear structures (Heiselberg *et al.* 1993; Lorenz *et al.* 1993).

Thus, for example, if the interface tension between quark and nuclear matter is sufficiently large, formation of a mixed phase is energetically unfavorable (Heiselberg *et al.* 1993). In this case, there is a first-order phase transition and the two phases coexist.

\*E-mail: anharutr@ysu.am

The neutron star will then have a core of pure quark matter and a crust of nuclear matter.

Because of uncertainty in the interface tension of strange quark matter, we presently cannot unambiguously establish which of the above alternatives is actually realized. Below, we consider the case that assumes an interface tension leading to a first-order phase transition with the possible coexistence of the two phases.

To study the functional dependence of the structural and integrated parameters of stellar configurations on the form of the equation of state for superdense matter, we have considered a large set of realistic equations of state that provide the coexistence of neutron matter with strange quark matter. We found that some of these equations of state gave rise to an additional local maximum in the dependence of stellar mass  $M$  on central stellar pressure  $P_c$  in a low-mass range ( $M/M_\odot \approx 0.08$ ); this provides the possible existence of a new family of stable equilibrium stellar configurations with interesting distinctive features. There is a quark core at the center of such stars, and the stellar radius can reach  $\sim 1000$  km, which makes them similar to white dwarfs.

Here, we report our results for one of such equations of state and focus our attention on the low-mass range.

## THE EQUATION OF STATE AND CALCULATIONS

The matter density inside a neutron star varies over a wide range, from several  $\text{g cm}^{-3}$  on the periphery (in the envelope) to  $10^{15} \text{ g cm}^{-3}$  at the center. At present, there is no unified theory that would faithfully describe the state of such matter with allowance for the formation of all possible constituents over the entire density range. Therefore, different equations of state are commonly used to construct the equation of state for neutron-star matter in different density ranges; of course, continuity is provided when passing from one range to another.

Here, we use the following equations of state for densities below the normal nuclear density:

$$7.86 \text{ g cm}^{-3} < \rho < 1.15 \times 10^3 \text{ g cm}^{-3}$$

(FMT, Feynman *et al.* 1949),

$$1.15 \times 10^3 \text{ g cm}^{-3} < \rho < 4.3 \times 10^{11} \text{ g cm}^{-3}$$

(BPS, Baym *et al.* 1971a).

Beginning from  $\rho_{nd} = 4.3 \times 10^{11} \text{ g cm}^{-3}$ , the matter composition changes, because neutrons are evaporated from nuclei: the so-called *Aen* structure is formed (the matter consists of nuclei, degenerate

neutrons and electrons), and the state is described by the equation

$$4.3 \times 10^{11} \text{ g cm}^{-3} < \rho < 2.21 \times 10^{13} \text{ g cm}^{-3}$$

(BBP, Baym *et al.* 1971b).

At subnuclear and supranuclear densities, we used the relativistic equation of state for neutron matter that was calculated by taking into account two-particle correlations based on the Bonn meson-exchange potential (Machleidt *et al.* 1987) and tabulated by Weber *et al.* (1991). We denoted this equation by GWG-Bonn:

$$3.56 \times 10^{13} \text{ g cm}^{-3} < \rho < 4.81 \times 10^{14} \text{ g cm}^{-3}$$

(GWG-Bonn, Weber *et al.* 1991).

These equations of state, which span the density range  $7.86 \text{ g cm}^{-3} < \rho < 4.81 \times 10^{14} \text{ g cm}^{-3}$ , describe the matter of a neutron star with a nucleon structure.

To study the phase transition, we must know the dependence of the baryon chemical potential  $\mu_B$  on pressure  $P$  or the function  $\varepsilon(n)$  and the dependence of the energy per baryon on baryon density  $n$ . To this end, we added the values of the following quantities to the tabulated values of  $P$ ,  $\rho$ , and  $n$ :

$$\mu_B(P) = n \frac{\partial(\rho c^2)}{\partial n} - \rho c^2 = \frac{P + \rho c^2}{n}, \quad (1)$$

$$\varepsilon(n) = \rho c^2 / n. \quad (2)$$

To describe the quark component, we used the quark-bag model developed at the Massachusetts Institute of Technology (MIT) by Chodos *et al.* (1974). According to this model, strange quark matter consists of quarks of three flavors,  $u$ ,  $d$ , and  $s$ , and of electrons that are in equilibrium relative to weak interactions. In our equation of state with a density discontinuity, the quark phase is described by phenomenological parameters of the bag model: the quark-gluon interaction constant  $\alpha_c = 0.5$ , the bag constant  $B = 55 \text{ MeV fm}^{-3}$ , and the strange quark mass  $m_s = 175 \text{ MeV}$ .

The Gibbs conditions

$$P^{(NM)} = P^{(QM)} = P_0, \quad (3)$$

$$\mu_B^{(NM)} = \mu_B^{(QM)}$$

yield the pressure  $P_0$ , the baryon densities  $n_N$  and  $n_Q$ , and the mass densities  $\rho_N$  and  $\rho_Q$ , which characterize the coexistence of the two phases [the superscripts  $(NM)$  and  $(QM)$  and the subscripts  $N$  and  $Q$  indicate that the quantities belong to the nucleon and quark phases, respectively].

The parameters of the first-order phase transition can also be determined by the standard Maxwell construction. For the first-order phase transition, the

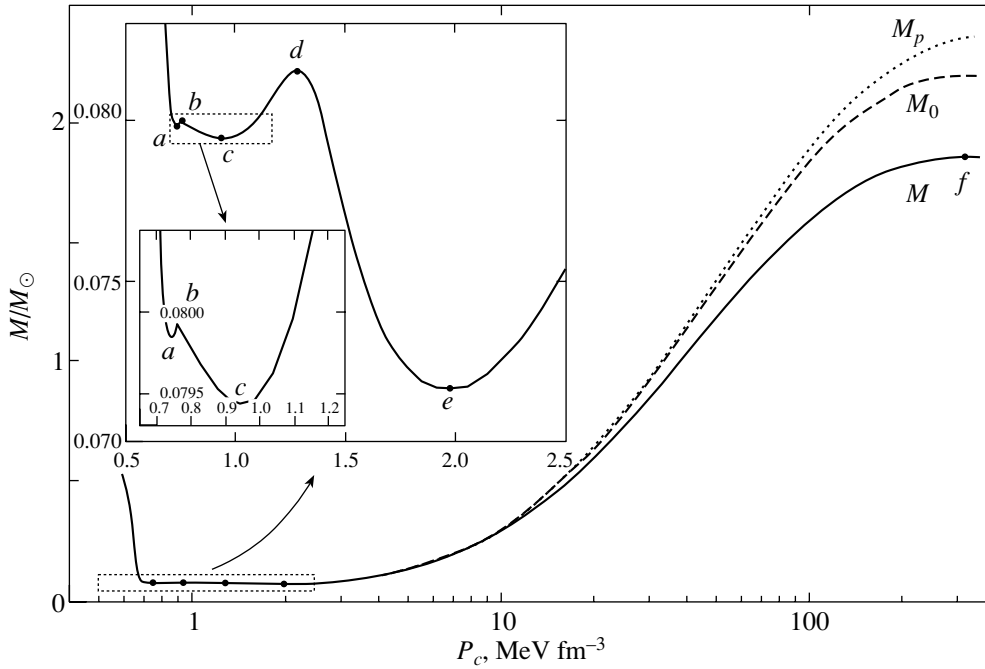


**Fig. 1.** Total mass  $M$ , rest mass  $M_0$ , and proper mass  $M_p$  versus central pressure. In the upper left corner, the dependence  $M(P_c)$  is shown for low masses on an enlarged scale. The symbols  $a, b, c, d, e, f$  denote critical configurations:  $a$  corresponds to an ordinary minimum-mass neutron star;  $b$  corresponds to the quark core formation threshold.

functional dependence of the energy per baryon satisfies the relations (similar to the Gibbs conditions)

$$\frac{\partial \varepsilon^{(NM)}}{\partial (1/n^{(NM)})} = \frac{\partial \varepsilon^{(QM)}}{\partial (1/n^{(QM)})} = -P_0, \quad (4)$$

$$\varepsilon_Q - \varepsilon_N = P_0 \left( \frac{1}{n_N} - \frac{1}{n_Q} \right),$$

$$\varepsilon_{N,Q} = \rho_{N,Q} c^2 / n_{N,Q},$$

which correspond to the common tangent in the plot of the energy per baryon  $\varepsilon$  against  $1/n$ .

Numerical calculations with this model yielded the following parameters of the first-order phase transition:  $P_0 = 0.76 \text{ MeV fm}^{-3}$ ,  $n_N = 0.12 \text{ fm}^{-3}$ ,  $n_Q = 0.26 \text{ fm}^{-3}$ ,  $\rho_N c^2 = 113.8 \text{ MeV fm}^{-3}$ ,  $\rho_Q c^2 = 250.5 \text{ MeV fm}^{-3}$ .

### MODELS OF NEUTRON STARS WITH A CORE OF STRANGE QUARK MATTER (HYBRID STARS): RESULTS AND DISCUSSION

The integrated parameters of a spherically symmetric static superdense star can be determined by numerically integrating the system of relativistic stellar-equilibrium equations (Tolman 1939; Oppenheimer and Volkoff 1939; Zel'dovich and Novikov 1971; Shapiro and Teukolsky 1983) supplemented with the equations for the relativistic moment of inertia (Hartle 1967) for a given equation of state  $\rho(P)$  and  $\rho_0(P)$  ( $\rho_0 = \frac{M(^{56}\text{Fe})}{56} n$  is the rest mass density, and  $n$  is the baryon number density).

The calculated gravitational mass  $M$ , rest mass  $M_0$ , and proper mass  $M_p$  are plotted against central pressure  $P_c$  in Fig. 1. Whereas these curves have an ordinary shape in the maximum-mass range (configuration  $f$ ), in the low-mass range, where the stability

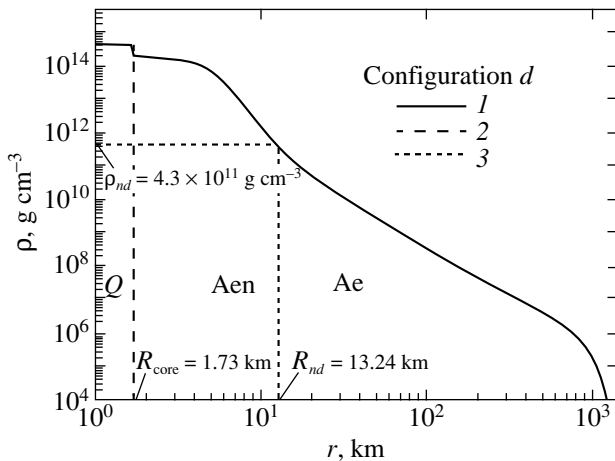


**Fig. 2.** Matter density  $\rho$  (1) versus radial coordinate  $r$  for configuration  $d$  (see Fig. 1 and the table); (2) the boundary of the strange quark core; (3) the  $A_{en}$  plasma formation threshold at  $\rho_{nd} = 4.3 \times 10^{11} \text{ g cm}^{-3}$ .

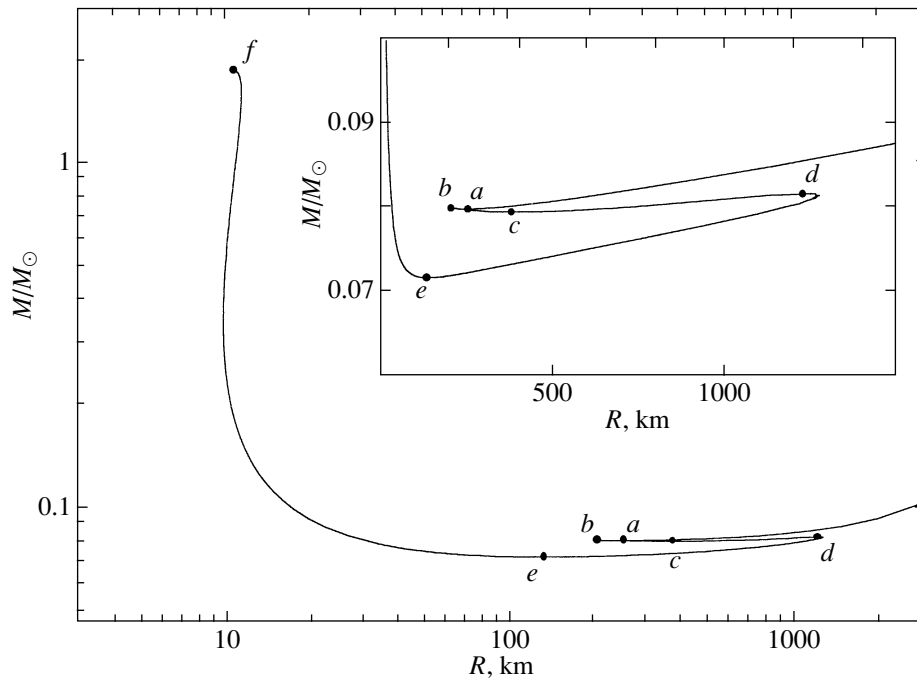


**Fig. 3.** Mass  $M$  of the star versus its radius  $R$ . In the upper right corner, the dependence  $M(R)$  is shown for small masses on an enlarged scale. The symbols  $a, b, c, d, e, f$  denote the same configurations as in Fig. 1.

is again lost—the condition  $dM/dP_c > 0$  is violated (configuration  $a$ )—there are several features that are absent for other equations of state. This range is shown on an enlarged scale in the upper left corner of the figure. Immediately after configuration  $a$ , there is a toothlike kink on the curve (configuration  $b$ ) attributable to the production of quarks. Segment  $ab$  corresponds to stable neutron stars without a quark core. The configurations with small quark cores are unstable (segment  $bc$  of the curve, where  $dM/dP_c < 0$ ). This is consistent with the results of Kaempfer (1981), who showed that if the condition

$$\lambda = \frac{\rho_Q}{\rho_N + P_0/c^2} > 3/2 \quad (5)$$

is satisfied, the configurations with a low-mass core of the new phase are unstable. In our case,  $\lambda = 2.19$ , which satisfies the above condition.

In general, when condition (5) is satisfied, the toothlike kink  $abc$  takes place on the ascending branch of the curve  $M(P_c)$  rather than in the low-mass range, and the curve monotonically rises after configuration  $c$  up to the maximum-mass configuration  $f$ . In our case, a local maximum is formed immediately after this kink again in the low-mass range—configuration  $d$ , for which the radius  $R$  exceeds a thousand kilometers and the mass slightly exceeds the mass of configuration  $b$  and is equal to  $0.082M_\odot$ . For this configuration, together with the

radius, the moment of inertia  $I$  also has a pronounced maximum (see the table and Fig. 5).

The table lists the basic parameters of critical configurations  $a, b, c, d, e, f$  ( $M_{\text{core}}$  and  $R_{\text{core}}$  are the core mass and radius, respectively). Also given here is the packing factor  $\alpha$ . For all critical configurations, this quantity is positive and (except for configuration  $f$ ) of the same order of magnitude as for white dwarfs.

Figure 2 shows a plot of matter density  $\rho$  against coordinate  $r$  ( $l$ ) for configuration  $d$ . Curve 2 indicates the boundary of the strange quark core, and curve 3 corresponds to the threshold of neutron evaporation from nuclei (the *Aen* plasma boundary). There is a density discontinuity ( $\rho_Q c^2 = 250.5 \text{ MeV fm}^{-3}$ ,  $\rho_N c^2 = 113.8 \text{ MeV fm}^{-3}$ ) at the quark core boundary.

As follows from our calculations, the radial coordinate  $R_{nd} = 13.24 \text{ km}$  and the accumulated mass  $M_{nd} = 0.07M_\odot$  correspond to the *Aen* plasma formation threshold. This configuration is similar in size to a white dwarf, but the bulk of its mass is concentrated in *Aen* plasma.

Figure 3 shows a plot of the stellar mass  $M$  against the stellar radius  $R$ . The symbols  $a, b, c, d, e, f$  denote the same configurations as in Fig. 1. As we see from Fig. 3, the equal-mass stars that correspond to branches  $cd$  and  $ef$  differ greatly in radius. While the stars of branch  $ef$  have radii  $\sim 10 \text{ km}$ , the stars of branch  $cd$  have large radii  $\sim 1000 \text{ km}$ , typical of white dwarfs.

Parameters of critical configurations

Configurations	$P_c, \text{MeV fm}^{-3}$	$\frac{M}{M_\odot}$	$R, \text{km}$	$\alpha = \frac{M_0 - M}{M_0}$	$I, M_\odot \text{ km}^2$	$\frac{M_{\text{core}}}{M_\odot}$	$R_{\text{core}}, \text{km}$
<i>a</i>	0.74	0.0798	254.7	0.00573	9.99	0	0
<i>b</i>	0.76	0.080	205	0.00597	6.6	0	0
<i>c</i>	0.94	0.079	380	0.00576	25.4	0.001	1.0
<i>d</i>	1.3	0.082	1251	0.00622	861.4	0.005	1.73
<i>e</i>	1.97	0.072	133.2	0.00596	2.4	0.016	2.59
<i>f</i>	321	1.86	10.8	0.15495	94.1	1.85	10.26

In Fig. 4, stellar radius  $R$  and quark-core radius  $R_{\text{core}}$  are plotted against central pressure  $P_c$  ( $I$ ). Curve 2 corresponds to neutron stars without quark cores. The dependence of quark-core radius on central pressure is represented by curve 3; curve 4 shows the distance from the stellar center to the threshold point, where, at  $\rho_{nd} = 4.3 \times 10^{11} \text{ g cm}^{-3}$ , *Aen* plasma is formed through the evaporation of neutrons from nuclei. A pronounced maximum is observed in the region of configuration *d*.

In Fig. 5, the relativistic moment of inertia  $I$  is plotted against central pressure  $P_c$ .

It should be noted that for the equation of state under consideration, accretion onto a neutron star

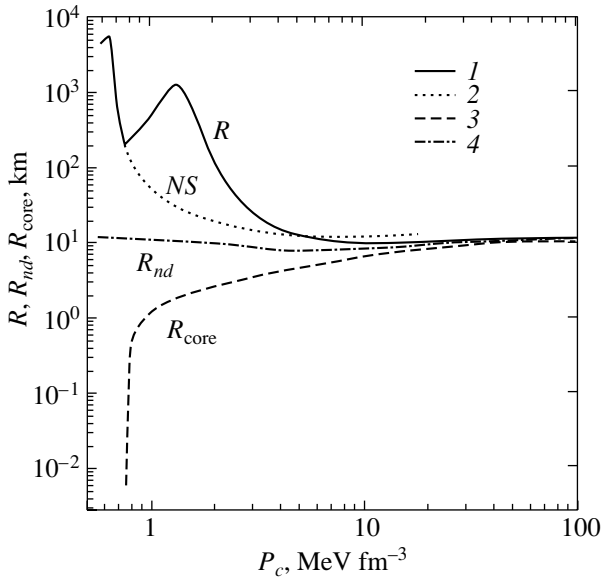


**Fig. 4.** (*I*) Stellar radius  $R$  versus central pressure  $P_c$ . Line (2) corresponds to ordinary neutron stars without quark cores; line (4) represents the  $P_c$  dependence of the quark core radius  $R_{\text{core}}$ ; and line (4) represents the dependence of coordinate  $R_{nd}$  that corresponds to the *Aen* plasma formation threshold.

will lead to two successive jumplike transitions to a quark-core neutron star; as a result, there will be two successive energy releases. First, a quark-core star that belongs to branch *cd* is formed; the subsequent accretion will lead to configurations with a radius of  $\sim 1000 \text{ km}$ , and, finally, a star of branch *ef* with a radius of  $\sim 100 \text{ km}$  is formed after the second catastrophic restructuring.

To establish whether our result is regular and that the additional (though mildly pronounced) maximum on the  $M(P_c)$  curve does not appear by chance, we considered several test equations of state for neutron matter that differ from our equation in a range close to the quark phase formation threshold. Our studies confirmed the regularity of the result and showed that, in some cases, varying the equation of state in the range  $9 \times 10^{13} < \rho < 1.8 \times 10^{14} \text{ g cm}^{-3}$  can even enhance the features found on the  $M(P_c)$  curve.

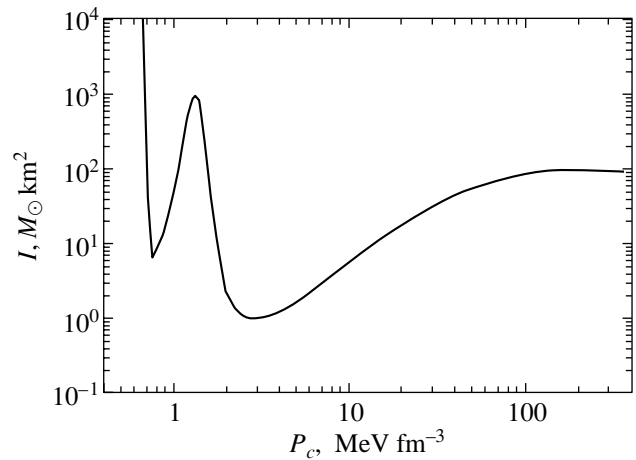


**Fig. 5.** Relativistic moment of inertia  $I$  versus central pressure.

## CONCLUSIONS

The first-order phase transition from the nucleon component to the strange quark state with a transition parameter  $\lambda > 3/2$  that occurs in superdense nuclear matter generally gives rise to a small tooth-like kink on the stable branch of the dependence of stellar mass on central pressure [curve  $M(P_c)$ ]. In our model, where the loss of stability in the low-mass range (the violation of condition  $dM/dP_c > 0$ ) takes place at higher densities than in other models ( $\rho_c = 2 \times 10^{14}$  g cm<sup>-3</sup>, the table, configuration *a*) and adjoins the quark production threshold ( $\rho_c = 4.5 \times 10^{14}$  g cm<sup>-3</sup>, the table, configuration *b*), a new local maximum emerges. This maximum leads to the possible existence of superdense low-mass stars with a radius of more than a thousand kilometers and with a kilometer-size quark core, in which a mere 6% of the total stellar mass is concentrated. Such stars are similar in size to white dwarfs, and the bulk of their mass is concentrated in *Aen* plasma.

## ACKNOWLEDGMENT

This study was carried out as part of topic no. 2000-55 supported by the Ministry of Education and Science of the Republic of Armenia.

## REFERENCES

1. G. B. Alaverdyan, A. R. Arutyunyan, Yu. L. Vartanyan, and A. K. Grigoryan, Dokl. Akad. Nauk Arm. **95**, 98 (1995).
2. C. Alcock, E. Farhi, and A. Olinto, Astrophys. J. **310**, 261 (1986).
3. G. Baym, C. Pethick, and P. Sutherland, Astrophys. J. **170**, 299 (1971a).
4. G. Baym, H. A. Bethe, and C. J. Pethick, Nucl. Phys. A **175**, 225 (1971b).
5. P. A. Carinhas, Astrophys. J. **412**, 213 (1993).
6. A. Chodos, R. L. Jaffe, K. Johnson, *et al.*, Phys. Rev. D **9**, 3471 (1974).
7. E. Farhi and R. L. Jaffe, Phys. Rev. D **30**, 2379 (1984).
8. R. P. Feynman, N. Metropolis, and E. Teller, Phys. Rev. **75**, 1561 (1949).
9. N. K. Glendenning, Phys. Rev. D **46**, 1274 (1992).
10. N. K. Glendenning, astro-ph/9706236 (1997).
11. P. Haensel, J. L. Zdunik, and R. Schaeffer, Astron. Astrophys. **160**, 121 (1986).
12. J. B. Hartle, Astrophys. J. **150**, 1005 (1967).
13. H. Heiselberg and M. Hjorth-Jensen, nucl-th/9902033 (1999).
14. H. Heiselberg, C. J. Pethick, and E. F. Staubo, Phys. Rev. Lett. **70**, 1355 (1993).
15. B. Kaempfer, Phys. Lett. B **101B**, 366 (1981).
16. S. B. Khadkikar, A. Mashra, and H. Mishra, Mod. Phys. Lett. **10**, 2651 (1995).
17. L. A. Kondratyuk, M. I. Krivoruchenko, and B. V. Martem'yanov, Pis'ma Astron. Zh. **16**, 954 (1990) [Sov. Astron. Lett. **16**, 410 (1990)].
18. C. P. Lorenz, D. G. Ravenhall, and C. J. Pethick, Phys. Rev. Lett. **70**, 379 (1993).
19. R. Machleidt, K. Holinde, and Ch. Elster, Phys. Rep. **149**, 1 (1987).
20. B. V. Martem'yanov, Pis'ma Astron. Zh. **20**, 588 (1994) [Astron. Lett. **20**, 499 (1994)].
21. J. R. Oppenheimer and G. M. Volkoff, Phys. Rev. **55**, 374 (1939).
22. S. L. Shapiro and S. A. Teukolsky, *Black Holes, White Dwarfs, and Neutron Stars: The Physics of Compact Objects* (Wiley, New York, 1983; Mir, Moscow, 1985).
23. R. C. Tolman, Phys. Rev. **55**, 364 (1939).
24. Yu. L. Vartanyan, A. R. Arutyunyan, and A. K. Grigoryan, Pis'ma Astron. Zh. **21**, 136 (1995) [Astron. Lett. **21**, 122 (1995)].
25. F. Weber and N. K. Glendenning, LBL-33066 (1992).
26. F. Weber, N. K. Glendenning, and M. K. Weigel, Astrophys. J. **373**, 579 (1991).
27. E. Witten, Phys. Rev. D **30**, 272 (1984).
28. Ya. B. Zel'dovich and I. D. Novikov, *Gravitational Theory and Stellar Evolution* (Nauka, Moscow, 1971).

*Translated by G. Rudnitskiĭ*